



UvA-DARE (Digital Academic Repository)

Inclusive search for the charmless radiative decay of the b quark ($b \rightarrow s \gamma$)

Adriani, O.; Aguilar-Benitez, M.; Ahlen, S.P.; Alcaraz, J.; Aloisio, A.; Alverson, G.; Alviggi, M.G.; Ambrosi, G.; Linde, F.L.

Published in:
Physics Letters B

DOI:
[10.1016/0370-2693\(93\)91384-Y](https://doi.org/10.1016/0370-2693(93)91384-Y)

[Link to publication](#)

Citation for published version (APA):

Adriani, O., Aguilar-Benitez, M., Ahlen, S. P., Alcaraz, J., Aloisio, A., Alverson, G., ... Linde, F. L. (1993). Inclusive search for the charmless radiative decay of the b quark ($b \rightarrow s \gamma$). *Physics Letters B*, 317, 637-646. DOI: 10.1016/0370-2693(93)91384-Y

General rights

It is not permitted to download or to forward/distribute the text or part of it without the consent of the author(s) and/or copyright holder(s), other than for strictly personal, individual use, unless the work is under an open content license (like Creative Commons).

Disclaimer/Complaints regulations

If you believe that digital publication of certain material infringes any of your rights or (privacy) interests, please let the Library know, stating your reasons. In case of a legitimate complaint, the Library will make the material inaccessible and/or remove it from the website. Please Ask the Library: <http://uba.uva.nl/en/contact>, or a letter to: Library of the University of Amsterdam, Secretariat, Singel 425, 1012 WP Amsterdam, The Netherlands. You will be contacted as soon as possible.

Inclusive search for the charmless radiative decay of the b -quark ($b \rightarrow s\gamma$)

L3 Collaboration

O. Adriani^o, M. Aguilar-Benitez^x, S. Ahlenⁱ, J. Alcaraz^p, A. Aloisio^{aa}, G. Alverson^j,
M.G. Alviggi^{aa}, G. Ambrosi^{af}, Q. An^q, H. Anderhub^{at}, A.L. Andersonⁿ, V.P. Andreev^{aj},
T. Angelescu^k, L. Antonov^{an}, D. Antreasyan^g, P. Arce^x, A. Arefiev^z, A. Atamanchuk^{aj},
T. Azemoon^c, T. Aziz^h, P.V.K.S. Baba^q, P. Bagnaia^{ai}, J.A. Bakken^{ah}, R.C. Ball^c, S. Banerjee^h,
J. Bao^e, R. Barillère^p, L. Barone^{ai}, A. Baschirotto^y, R. Battiston^{af}, A. Bay^r, F. Becattini^o,
J. Bechtluft^a, R. Becker^a, U. Becker^{n,at}, F. Behner^{at}, J. Behrens^{at}, Gy.L. Bencze^l, J. Berdugo^x,
P. Bergesⁿ, B. Bertucci^{af}, B.L. Betev^{an,at}, M. Biasini^{af}, A. Biland^{at}, G.M. Bilei^{af}, R. Bizzarri^{ai},
J.J. Blaising^d, G.J. Bobbink^{p,b}, R. Bock^a, A. Böhm^a, B. Borgia^{ai}, M. Bosetti^y, D. Bourilkov^{ac},
M. Bourquin^r, D. Boutigny^p, B. Bouwens^b, E. Brambilla^{aa}, J.G. Branson^{ak}, I.C. Brock^{ag},
M. Brooks^v, A. Bujak^{aq}, J.D. Burgerⁿ, W.J. Burger^r, J. Busenitz^{ap}, A. Buytenhuijs^{ac}, X.D. Cai^q,
M. Capellⁿ, M. Caria^{af}, G. Carlino^{aa}, A.M. Cartacci^o, R. Castello^y, M. Cerrada^x, F. Cesaroni^{ai},
Y.H. Changⁿ, U.K. Chaturvedi^q, M. Chemarin^w, A. Chen^{av}, C. Chen^f, G. Chen^f, G.M. Chen^f,
H.F. Chen^s, H.S. Chen^f, M. Chenⁿ, W.Y. Chen^{av}, G. Chiefari^{aa}, C.Y. Chien^e, M.T. Choi^{ao},
S. Chungⁿ, C. Civinini^o, I. Clareⁿ, R. Clareⁿ, T.E. Coan^v, H.O. Cohn^{ad}, G. Coignet^d,
N. Colino^p, A. Contin^g, F. Cotorobai^k, X.T. Cui^q, X.Y. Cui^q, T.S. Daiⁿ, R. D'Alessandro^o,
R. de Asmundis^{aa}, A. Degré^d, K. Deiters^{ar}, E. Dénes^l, P. Denes^{ah}, F. DeNotaristefani^{ai},
M. Dhina^{at}, D. DiBitonto^{ap}, M. Diemoz^{ai}, H.R. Dimitrov^{an}, C. Dionisi^{ai}, M. Dittmar^{at},
L. Djambazov^{at}, M.T. Dova^q, E. Drago^{aa}, D. Duchesneau^r, P. Duinker^b, I. Duran^{al}, S. Easo^{af},
H. El Mamouni^w, A. Engler^{ag}, F.J. Epplingⁿ, F.C. Erné^b, P. Extermann^r, R. Fabbretti^{ar},
M. Fabre^{ar}, S. Falciano^{ai}, S.J. Fan^{am}, O. Fackler^u, J. Fay^w, M. Felcini^p, T. Ferguson^{ag},
D. Fernandez^x, G. Fernandez^x, F. Ferroni^{ai}, H. Fesefeldt^a, E. Fiandrini^{af}, J.H. Field^r,
F. Filthaut^{ac}, G. Finocchiaro^{ai}, P.H. Fisher^e, G. Forconi^r, L. Fredj^r, K. Freudenreich^{at},
W. Friebel^{as}, M. Fukushimaⁿ, M. Gailloud^t, Yu. Galaktionov^{z,n}, E. Gallo^o, S.N. Ganguli^{p,h},
P. Garcia-Abia^x, D. Gele^w, S. Gentile^{ai}, N. Gheordanescu^k, S. Giagu^{ai}, S. Goldfarb^j,
Z.F. Gong^s, E. Gonzalez^x, A. Gougas^e, D. Goujon^r, G. Gratta^{ac}, M. Gruenewald^p, C. Gu^q,
M. Guanziroli^q, J.K. Guo^{am}, V.K. Gupta^{ah}, A. Gurtu^h, H.R. Gustafson^c, L.J. Gutay^{aq},
K. Hangarter^a, B. Hartmann^a, A. Hasan^q, D. Hauschildt^b, C.F. He^{am}, J.T. He^f, T. Hebbeker^p,
M. Hebert^{ak}, A. Hervé^p, K. Hilgers^a, H. Hofer^{at}, H. Hoorani^r, G. Hu^q, G.Q. Hu^{am}, B. Ille^w,
M.M. Ilyas^q, V. Innocente^p, H. Janssen^p, S. Jezequel^d, B.N. Jin^f, L.W. Jones^c,
I. Josa-Mutuberría^p, A. Kasser^t, R.A. Khan^q, Yu. Kamyshkov^{ad}, P. Kapinos^{aj,as},
J.S. Kapustinsky^v, Y. Karyotakis^p, M. Kaur^q, S. Khokhar^q, M.N. Kienzle-Focacci^r,
J.K. Kim^{ao}, S.C. Kim^{ao}, Y.G. Kim^{ao}, W.W. Kinnison^v, A. Kirkby^{ac}, D. Kirkby^{ac}, S. Kirsch^{as},
W. Kittel^{ac}, A. Klimentov^{n,z}, R. Klöckner^a, A.C. König^{ac}, E. Koffeman^b, O. Kornadt^a,
V. Koutsenko^{n,z}, A. Koulbardis^{aj}, R.W. Kraemer^{ag}, T. Kramerⁿ, V.R. Krastev^{an,af}, W. Krenz^a,
A. Krivshich^{aj}, H. Kuijten^{ac}, K.S. Kumar^m, A. Kunin^{n,z}, G. Landi^o, D. Lanske^a, S. Lanzano^{aa},
A. Lebedevⁿ, P. Lebrun^w, P. Lecomte^{at}, P. Lecoq^p, P. Le Coultre^{at}, D.M. Lee^v, J.S. Lee^{ao},
K.Y. Lee^{ao}, I. Leedom^j, C. Leggett^c, J.M. Le Goff^p, R. Leiste^{as}, M. Lenti^o, E. Leonardi^{ai},
C. Li^{s,q}, H.T. Li^f, P.J. Li^{am}, J.Y. Liao^{am}, W.T. Lin^{av}, Z.Y. Lin^s, F.L. Linde^b, B. Lindemann^a,

L. Lista^{aa}, Y. Liu^q, W. Lohmann^{as}, E. Longo^{ai}, Y.S. Lu^f, J.M. Lubbers^p, K. Lübelmeyer^a, C. Luci^{ai}, D. Luckey^{gn}, L. Ludovici^{ai}, L. Luminari^{ai}, W. Luster^{as}, J.M. Ma^f, W.G. Ma^s, M. MacDermott^{at}, R. Malik^q, A. Malinin^z, C. Maña^x, M. Maolinbay^{at}, P. Marchesini^{at}, F. Marion^d, A. Marinⁱ, J.P. Martin^w, L. Martinez-Laso^x, F. Marzano^{ai}, G.G.G. Massaro^b, K. Mazumdar^r, P. McBride^m, T. McMahon^{aq}, D. McNally^{at}, M. Merk^{ag}, L. Merola^{aa}, M. Meschini^o, W.J. Metzger^{ac}, Y. Mi^t, A. Mihul^k, G.B. Mills^v, Y. Mir^q, G. Mirabelli^{ai}, J. Mnich^a, M. Möller^a, B. Monteleoni^o, R. Morand^d, S. Morganti^{ai}, N.E. Moulai^q, R. Mount^{ae}, S. Müller^a, A. Nadtochy^{aj}, E. Nagy^l, M. Napolitano^{aa}, F. Nessi-Tedaldi^{at}, H. Newman^{ae}, C. Neyer^{at}, M.A. Niaz^q, A. Nippe^a, H. Nowak^{as}, G. Organtini^{ai}, D. Pandoulas^a, S. Paoletti^o, P. Paolucci^{aa}, G. Pascale^{ai}, G. Passaleva^{o,af}, S. Patricelli^{aa}, T. Paul^e, M. Pauluzzi^{af}, C. Paus^a, F. Pauss^{at}, Y.J. Pei^a, S. Pensotti^y, D. Perret-Gallix^d, J. Perrier^r, A. Pevsner^e, D. Piccolo^{aa}, M. Pieri^p, P.A. Piroué^{ah}, F. Plasil^{ad}, V. Plyaskin^z, M. Pohl^{at}, V. Pojidaev^{zo}, H. Postemaⁿ, Z.D. Qi^{am}, J.M. Qian^c, K.N. Qureshi^q, R. Raghavan^h, G. Rahal-Callot^{at}, P.G. Rancoita^y, M. Rattaggi^y, G. Raven^b, P. Razis^{ab}, K. Read^{ad}, D. Ren^{at}, Z. Ren^q, M. Rescigno^{ai}, S. Reucroft^j, A. Ricker^a, S. Riemann^{as}, B.C. Riemers^{aq}, K. Riles^c, O. Rind^c, H.A. Rizvi^q, S. Ro^{ao}, F.J. Rodriguez^x, B.P. Roe^c, M. Röhner^a, L. Romero^x, S. Rosier-Lees^d, R. Rosmalen^{ac}, Ph. Rosselet^t, W. van Rossum^b, S. Roth^a, A. Rubbiaⁿ, J.A. Rubio^p, H. Rykaczewski^{at}, M. Sachwitz^{as}, J. Salicio^p, J.M. Salicio^x, G.S. Sanders^v, A. Santocchia^{af}, M.S. Sarakinosⁿ, G. Sartorelli^{g,q}, M. Sassowsky^a, G. Sauvage^d, V. Schegelsky^{aj}, D. Schmitz^a, P. Schmitz^a, M. Schneegans^d, H. Schopper^{au}, D.J. Schotanus^{ac}, S. Shotkinⁿ, H.J. Schreiber^{as}, J. Shukla^{ag}, R. Schulte^a, S. Schulte^a, K. Schultze^a, J. Schwenke^a, G. Schwering^a, C. Sciacca^{aa}, I. Scott^m, R. Sehgal^q, P.G. Seiler^{ar}, J.C. Sens^{p,b}, L. Servoli^{af}, I. Sheer^{ak}, D.Z. Shen^{am}, S. Shevchenko^{ae}, X.R. Shi^{ae}, E. Shumilov^z, V. Shoutko^z, D. Son^{ao}, A. Sopczak^{ak}, C. Spartiotis^e, T. Spickermann^a, P. Spillantini^o, R. Starosta^a, M. Steuer^{gn}, D.P. Stickland^{ah}, F. Sticozziⁿ, H. Stone^{ah}, K. Strauch^m, B.C. Stringfellow^{aq}, K. Sudhakar^h, G. Sultanov^q, L.Z. Sun^{s,q}, G.F. Susinno^r, H. Suter^{at}, J.D. Swain^q, A.A. Syed^{ac}, X.W. Tang^f, L. Taylor^j, G. Terzi^y, Samuel C.C. Tingⁿ, S.M. Tingⁿ, M. Tonutti^a, S.C. Tonwar^h, J. Tóth^l, A. Tsaregorodtsev^{aj}, G. Tsiopolitis^{ag}, C. Tully^{ah}, K.L. Tung^f, J. Ulbricht^{at}, L. Urbán^l, U. Uwer^a, E. Valente^{ai}, R.T. Van de Walle^{ac}, I. Vetlitsky^z, G. Viertel^{at}, P. Vikas^q, U. Vikas^q, M. Vivargent^d, H. Vogel^{ag}, H. Vogt^{as}, I. Vorobiev^z, A.A. Vorobyov^{aj}, L. Vuilleumier^t, M. Wadhwa^d, W. Wallraff^a, C. Wangⁿ, C.R. Wang^s, X.L. Wang^s, Y.F. Wangⁿ, Z.M. Wang^{q,s}, C. Warner^a, A. Weber^a, J. Weber^{at}, R. Weill^t, T.J. Wenaus^u, J. Wenninger^f, M. Whiteⁿ, C. Willmott^x, F. Wittgenstein^p, D. Wright^{ah}, S.X. Wu^q, S. Wynhoff^a, B. Wysłouchⁿ, Y.Y. Xie^{am}, J.G. Xu^f, Z.Z. Xu^s, Z.L. Xue^{am}, D.S. Yan^{am}, B.Z. Yang^s, C.G. Yang^f, G. Yang^q, C.H. Ye^q, J.B. Ye^s, Q. Ye^q, S.C. Yeh^{av}, Z.W. Yin^{am}, J.M. You^q, N. Yunus^q, M. Yzerman^b, C. Zaccardelli^{ae}, P. Zemp^{at}, M. Zeng^q, Y. Zeng^a, D.H. Zhang^b, Z.P. Zhang^{s,q}, B. Zhouⁱ, G.J. Zhou^f, J.F. Zhou^a, R.Y. Zhu^{ae}, A. Zichichi^{g,p,q} and B.C.C. van der Zwaan^b

^a I. Physikalisches Institut, RWTH, W-5100 Aachen, FRG¹

and III. Physikalisches Institut, RWTH, W-5100 Aachen, FRG¹

^b National Institute for High Energy Physics, NIKHEF, NL-1009 DB Amsterdam, The Netherlands

^c University of Michigan, Ann Arbor, MI 48109, USA

^d Laboratoire d'Annecy-le-Vieux de Physique des Particules, LAPP, IN2P3-CNRS, BP 110, F-74941 Annecy-le-Vieux Cedex, France

^e Johns Hopkins University, Baltimore, MD 21218, USA

^f Institute of High Energy Physics, IHEP, 100039 Beijing, China

^g INFN - Sezione di Bologna, I-40126 Bologna, Italy

^h Tata Institute of Fundamental Research, Bombay 400 005, India

ⁱ Boston University, Boston, MA 02215, USA

- ^j Northeastern University, Boston, MA 02115, USA
^k Institute of Atomic Physics and University of Bucharest, R-76900 Bucharest, Romania
^l Central Research Institute for Physics of the Hungarian Academy of Sciences, H-1525 Budapest 114, Hungary²
^m Harvard University, Cambridge, MA 02139, USA
ⁿ Massachusetts Institute of Technology, Cambridge, MA 02139, USA
^o INFN – Sezione di Firenze and University of Florence, I-50125 Florence, Italy
^p European Laboratory for Particle Physics, CERN, CH-1211 Geneva 23, Switzerland
^q World Laboratory, FBLJA Project, CH-1211 Geneva 23, Switzerland
^r University of Geneva, CH-1211 Geneva 4, Switzerland
^s Chinese University of Science and Technology, USTC, Hefei, Anhui 230 029, China
^t University of Lausanne, CH-1015 Lausanne, Switzerland
^u Lawrence Livermore National Laboratory, Livermore, CA 94550, USA
^v Los Alamos National Laboratory, Los Alamos, NM 87544, USA
^w Institut de Physique Nucléaire de Lyon, IN2P3-CNRS, Université Claude Bernard, F-69622 Villeurbanne Cedex, France
^x Centro de Investigaciones Energeticas, Medioambientales y Tecnológicas, CIEMAT, E-28040 Madrid, Spain
^y INFN – Sezione di Milano, I-20133 Milan, Italy
^z Institute of Theoretical and Experimental Physics, ITEP, Moscow, Russia
^{aa} INFN – Sezione di Napoli and University of Naples, I-80125 Naples, Italy
^{ab} Department of Natural Sciences, University of Cyprus, Nicosia, Cyprus
^{ac} University of Nymegen and NIKHEF, NL-6525 ED Nymegen, The Netherlands
^{ad} Oak Ridge National Laboratory, Oak Ridge, TN 37831, USA
^{ae} California Institute of Technology, Pasadena, CA 91125, USA
^{af} INFN-Sezione di Perugia and Università Degli Studi di Perugia, I-06100 Perugia, Italy
^{ag} Carnegie Mellon University, Pittsburgh, PA 15213, USA
^{ah} Princeton University, Princeton, NJ 08544, USA
^{ai} INFN-Sezione di Roma and University of Rome, “La Sapienza”, I-00185 Rome, Italy
^{aj} Nuclear Physics Institute, St. Petersburg, Russia
^{ak} University of California, San Diego, CA 92093, USA
^{al} Departamento de Física de Partículas Elementales, Universidad de Santiago, E-15706 Santiago de Compostela, Spain
^{am} Shanghai Institute of Ceramics, SIC, Shanghai, China
^{an} Bulgarian Academy of Sciences, Institute of Mechatronics, BU-1113 Sofia, Bulgaria
^{ao} Center for High Energy Physics, Korea Advanced Institute of Sciences and Technology, 305-701 Taejeon, South Korea
^{ap} University of Alabama, Tuscaloosa, AL 35486, USA
^{aq} Purdue University, West Lafayette, IN 47907, USA
^{ar} Paul Scherrer Institut, PSI, CH-5232 Villigen, Switzerland
^{as} DESY-Institut für Hochenergiephysik, O-1615 Zeuthen, FRG
^{at} Eidgenössische Technische Hochschule, ETH Zürich, CH-8093 Zürich, Switzerland
^{au} University of Hamburg, W-2000 Hamburg, FRG
^{av} High Energy Physics Group, Taiwan, ROC

Received 22 July 1993

Editor: K. Winter

We report on the search for the electromagnetic penguin decay $b \rightarrow s\gamma$ at $\sqrt{s} \approx m_Z$. We find no evidence for a signal and place an upper limit on the decay rate $\text{Br}(b \rightarrow s\gamma) < 1.2 \times 10^{-3}$ at 90% C.L.

1. Introduction

The electromagnetic penguin b decay $b \rightarrow s\gamma$ [1] is a flavor changing neutral current transition induced at leading order by one-loop diagrams with a W boson propagator and u, c, t quarks in the loop. Within the Standard Model [2], the inclusive branching ra-

¹ Supported by the German Bundesministerium für Forschung und Technologie.

² Supported by the Hungarian OTKA fund under contract number 2970.

tio $b \rightarrow s\gamma$ is expected to be $\text{Br}(b \rightarrow s\gamma) = (2.56-3.94) \times 10^{-4}$ for m_t in the range 90–200 GeV [3]. Electromagnetic penguin decays offer a unique window to probe new hypotheses [4,5] beyond the Standard Model. In particular, Two Higgs Doublets [6] theories contain new diagrams with a charged Higgs boson that add constructively to the W boson loop diagram. The dominant contribution of the t -quark loop make the $b \rightarrow s\gamma$ transition particularly sensitive to the Htb vertex. A possible enhancement in the $b \rightarrow s\gamma$ decay rate could be interpreted as a signal for new physics. In the Minimal Supersymmetric extension of the Standard Model (MSSM) [7] where there could be destructive contributions from superpartners, the decay rate could be larger or smaller [5] than in the Standard Model depending on the choice of model parameters.

Because of the large mass of the b -quark, the properties of the electromagnetic penguin decay of a b -hadron are mainly governed by the $b \rightarrow s\gamma$ decay. Exclusive decay channels of the B mesons are the two body decays $B_d^0 \rightarrow \mathcal{K}^0\gamma$ and $B^+ \rightarrow \mathcal{K}^+\gamma$, where \mathcal{K} is a strange resonance and $B_s^0 \rightarrow \phi\gamma$. Early searches for the B_d^0 and B^\pm penguin decays were undertaken by the ARGUS, CLEO and CRYSTAL BALL collaborations [8]. The first candidates of the $B^0 \rightarrow K^{*0}(892)\gamma$ and $B^- \rightarrow K^{*-}(892)\gamma$ decays were recently reported by the CLEO collaboration [9].

Although the quark level calculations for the $b \rightarrow s\gamma$ branching ratio are rather precise, the predictions of the branching ratios for exclusive decay channels are affected by large uncertainties due to the long-distance QCD effects [4]. Therefore, the $b \rightarrow s\gamma$ inclusive decay rate cannot be exactly derived from the measurements of the exclusive decay branching ratios. The observation of the exclusive decays by the CLEO collaboration has however allowed to set the lower bound $\text{Br}(b \rightarrow s\gamma) > 0.6 \times 10^{-4}$ at 95% C.L. [9].

In this paper, we report on an inclusive search for the $b \rightarrow s\gamma$ decay at LEP based on an integrated luminosity of 37 pb^{-1} collected with the L3 detector during the 1991 and 1992 runs. The advantage of the inclusive search is that one can derive or set an upper limit on the $b \rightarrow s\gamma$ rate independently of the decay products of the b -hadron. The invariant mass of a system in the decay $B \rightarrow S\gamma$ is reconstructed independently of S by using the photon and jet axis kinematics. The signal is identified by requiring the

invariant mass of B be compatible with that of a b -hadron. The energy of the photon in the rest frame of B is reconstructed and used to further suppress the background. The calculation of the photon spectrum in the inclusive $b \rightarrow s\gamma$ decay [10] predicts this energy to be peaked towards $E_\gamma^{\text{max}} = (m_b^2 - m_s^2)/(2m_b)$, where m_b (m_s) is the mass of the b (s) quark.

The background to this search is dominated by prompt photons in hadronic Z decays and by energetic leading neutral mesons produced in fragmentation decaying to two unresolved photons.

2. L3 detector

Details of the L3 detector can be found in ref. [11]. L3 consists of a time expansion chamber (TEC) for tracking charged particles, a high resolution electromagnetic calorimeter of BGO crystals, a barrel of scintillation counters, a hadron calorimeter with uranium absorber and proportional wire chamber readout and a muon spectrometer. The luminosity is determined from small-angle Bhabha scattering using BGO electromagnetic calorimetry in the polar angle ranges θ and $\pi - \theta$ between 24.93 and 69.94 mrad. The fiducial solid angle is 99% of 4π . All subdetectors are installed inside a 12 m diameter solenoidal magnet which provides a uniform 0.5 T field along the beam direction.

3. Selection of hadronic events with a hard photon

The selection of hadronic events is based on the energy measured in the electromagnetic and hadronic calorimeters. Events are accepted if

$$0.5 < \frac{E_{\text{vis}}}{\sqrt{S}} < 1.5, \quad \frac{|E_{\parallel}|}{E_{\text{vis}}} < 0.5, \quad \frac{E_{\perp}}{E_{\text{vis}}} < 0.5,$$

$$N_{\text{cluster}} > 16, \quad N_{\text{tracks}} > 4,$$

where E_{vis} is the total energy observed in the calorimeters, E_{\parallel} is the energy imbalance along the beam direction, and E_{\perp} is the transverse energy imbalance. The clusters are constructed by grouping neighboring calorimeter signals which are likely to be produced by the same particle. The cut on the number of clusters and number of tracks selects only high multiplicity events. We collected 927772 such events during the 1991 and 1992 runs. The acceptance of the

cuts for hadronic Z decays is determined with the JETSET [12] Monte Carlo program to be $(95.28 \pm 0.04(\text{stat.}))\%$. The trigger efficiency for these events is better than 99.9% due to the combination of all the detector triggers. The contamination from $Z \rightarrow \tau^+ \tau^-$ decays is estimated to be about 430 events and is neglected.

Photons produced in multi-hadronic events are identified by analyzing the shape of the electromagnetic showers in the BGO calorimeter. The ratio of the energy deposited in a 3×3 crystal array (\sum_9) and a 5×5 array (\sum_{25}) around the most energetic crystal must satisfy $\sum_9 / \sum_{25} > 0.94$. Fully simulated multi-hadronic events indicate that in addition to prompt photons radiated from final-state quarks and to a lesser extent from initial-state photons (for which the \sqrt{s} dependence has been neglected), the selected events contain unresolved photon pairs from the decay of neutral hadrons (typically π^0 's or η 's). An algorithm which uses a chi-square method to compare the energy deposited in each crystal with the predicted energy of an electromagnetic shower is used to reduce this neutral mesons background. The cut $\chi^2 < 25$ is used to pre-select the electromagnetic clusters^{#1}. The behavior of the \sum_9 / \sum_{25} and χ^2 was checked with the Bhabha sample $e^+ e^- \rightarrow e^+ e^- (\gamma)$. The difference between data and Monte Carlo shows a systematic error of about 2%. To select neutral clusters, a charge veto requiring there be no track within $\Delta\phi = 5$ mrad half-opening angle around the cluster direction removes electrons and other charged particles.

For this search, hadronic events are selected if there is at least one hard photon with an energy greater than 10 GeV. This cut removes a large fraction of the background coming from radiated photons and from fragmentation into π^0 's or η 's since their energies have sharp falling spectrums. The photons are required to lie within the barrel region, $|\cos\theta| < 0.72$.

Fully simulated JETSET Monte Carlo events – ≈ 960 K events – are normalized to the number of hadronic events prior to electromagnetic cluster selection. The data and Monte Carlo samples are then subjected to the selection cuts. We obtain 25120 events from the data, while from the JETSET sample

$22628 \pm 152(\text{stat.})$ are expected, which is roughly 10% less. As a cross-check, about 380 K fully simulated events generated with the HERWIG Monte Carlo [13] are subjected to the same cuts. This yields 24506 ± 249 events which is consistent with the data.

The study of energetic isolated hard photon emission in hadronic events has been reported in ref. [14], where comparisons with theoretical models were presented. Uncertainties in the number of hard electromagnetic clusters are dominated by the description of the radiative process $Z \rightarrow q\bar{q}\gamma$ and by the fragmentation process which can yield single particles with energies up to the beam energy. The study of ref. [14] considers only isolated electromagnetic clusters. The angle of isolation ξ between low-energy π^0 's and η 's and the nearest jet axis^{#2} has been compared to the predictions of JETSET and HERWIG. In the region $\xi < 30^\circ$, discrepancies up to 10% are seen in the angle distribution. In this analysis, the JETSET sample is normalized to the data after the selection described above.

4. $b \rightarrow s\gamma$ selection

The background is highly suppressed with stringent photon identification cuts and by reconstructing the following three kinematical variables using calorimetric information: the mass of the b -hadron candidate, \hat{m}_b , the energy of the photon in the b -hadron rest frame, E_γ^* , and the direction of emission of the photon in the b rest frame with respect to the b direction of flight, θ^* .

The shapes of the \sum_9 / \sum_{25} and χ^2 distributions in the hadronic event agree well with those predicted by the JETSET Monte Carlo. The electromagnetic clusters must satisfy

- (1) $\chi^2 < 12$,
- (2) $\sum_9 / \sum_{25} > 0.99$.

After these cuts, 9272 events survive in the data and are in good agreement with the Monte Carlo expectations. In the rest of the selection, the direction of flight of the b -hadron is approximated by the event thrust axis, \mathbf{n}_{thr} . The simulation yields a Gaussian error on the direction of the b -hadron with a sigma of

^{#1} The χ^2 is found by summing over 9 crystals such that the DOF = 8.

^{#2} Jets are reconstructed using the JADE [15] algorithm with a $y_{\text{cut}} = 0.05$.

30.1 ± 0.1 mrad. The additional cut on the cosine of the polar of the thrust axis is applied:

$$(3) |\cos(\theta_{\text{thr}})| < 0.7.$$

In the laboratory frame, the b -hadron spans a large momentum spectrum peaked at high momenta, parametrized by the Peterson et al. formula [16] ($\epsilon_b = 0.050$ [17] is used). In the simulation of the fragmentation process, a correlation is seen between the momentum of the b -hadron and the charged multiplicity of the jet closest to the photon, k_j . By selecting events where the jet charged multiplicity is low, the sample is biased toward high energy b -hadrons, which helps restrict the energy spread. The following cut is used:

$$(4) k_j < 5,$$

which increases the mean energy of the selected b -hadrons by approximately 6 GeV and decreases the RMS by about 3 GeV. Some implications of cut (4) will be discussed when the efficiency for detecting the signal is calculated.

Kinematics are used to calculate the invariant mass of the b -hadron. The energy of the "jet" system J recoiling against the photon is computed by balancing the transverse momenta of the photon and of J with respect to the thrust axis. The direction of flight of the jet " J " is approximated by

$$\mathbf{p}_J = (m_B \sqrt{\gamma^2 - 1}) \mathbf{n}_{\text{thr}} - \mathbf{p}_\gamma, \quad (1)$$

where it is assumed that $\gamma = 6.6$ and $m_B = 5.3$ GeV. The same Lorentz boost is used for the rest of the analysis. Defining the angle between the thrust axis and the photon by θ_1 and the angle between the thrust axis and the jet " J " by θ_2 , i.e. $\cos \theta_1 = \mathbf{n}_{\text{thr}} \cdot \mathbf{p}_\gamma / |\mathbf{p}_\gamma|$, and $\cos \theta_2 = \mathbf{n}_{\text{thr}} \cdot \mathbf{p}_J / |\mathbf{p}_J|$, then, with the constraint on the jet energy, the invariant mass becomes

$$\hat{m}_b^2 = 2E_\gamma^2 \left(\frac{\sin \theta_1}{\sin \theta_2} \right) (1 - \cos(\theta_1 + \theta_2)), \quad (2)$$

which is independent of E_J . In the simulated events, the boost gives a resolution of $19.4 \pm 0.5\%$ for E_γ^* and the ratio of the energy measured to that generated has a mean of 1.022 ± 0.005 . A set of different Lorentz boosts ranging from 6 up to 8 were tested and no significant change of resolution resulted. The direction of flight of the photon in the b -hadron rest frame, $\cos \theta^*$, should reflect isotropic emission. The background which originates from the fragmentation

tends to be forward or backward to the direction of flight. To obtain θ^* , the photon candidate is boosted along the thrust axis assuming a boost of 6.6.

The distribution of $\cos(\theta^*)$ after cuts (1)–(4) is shown in fig. 1. The $\cos(\theta^*)$ distribution for the data is peaked at -1 and $+1$ while for the signal it is consistent with being flat. The data is not symmetrically distributed around $\cos(\theta^*) = 0$ as the cut on the energy reduces the efficiency for detecting photons backward to the direction of flight. To reduce further the background, the following cut is applied:

$$(5) -0.8 < \cos(\theta^*) < 0.5.$$

The distribution of E_γ^* and \hat{m}_b after cuts (1)–(5) are shown in figs. 2 and 3 for the data compared to the simulated background. For the signal, the \hat{m}_b distribution is expected to be centered at 5.3 GeV with a width of 1.2 GeV and the energy E_γ^* at 2.8 GeV. Therefore, events are selected if they satisfy

$$(6) 1.8 < E_\gamma^* < 3.8 \text{ GeV},$$

$$(7) 4 < \hat{m}_b < 7 \text{ GeV}.$$

The transverse momentum of the photon is calculated with respect to the thrust axis. The measured p_t which is smeared by the angular resolution of the thrust axis is used to remove background:

$$(8) p_t < 3.4 \text{ GeV}.$$

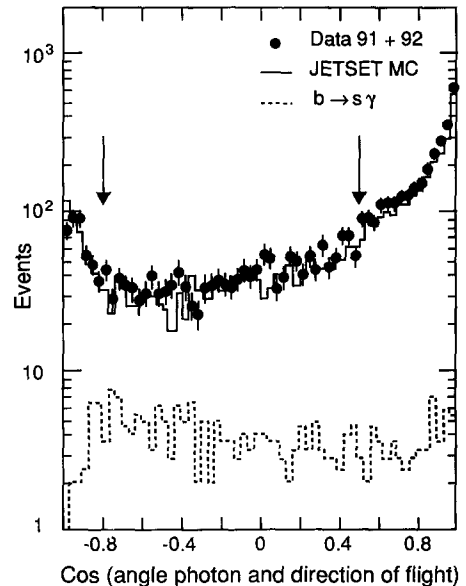


Fig. 1. The cosine of the angle between the photon and the thrust axis assuming a Lorentz boost of 6.6.

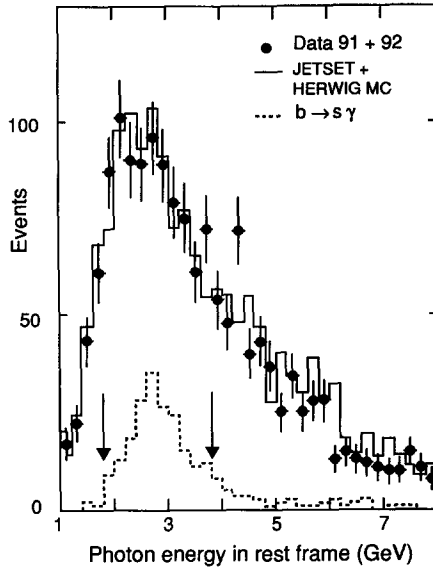


Fig. 2. Reconstructed photon energy in the B rest frame.

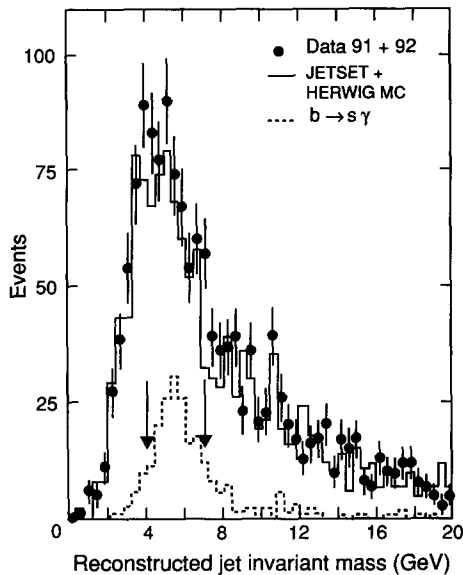


Fig. 3. Reconstructed invariant mass of the B meson candidate.

After all the cuts, 88 events are left in the data while 85.9 ± 9.0 (stat.) are expected from background. The contamination from π^0 and η amounts to 31.1 ± 5.5 (stat.) events in total. There is no evidence for a signal in the data. For example, the distribution of the photon energy E_γ^* is compatible with a flat distribu-

tion. The bin-by-bin difference between the data and the Monte Carlo for this variable is taken and a horizontal straight line is fitted with constant 0.43 ± 0.36 and a chi-square $\chi^2 = 37.45$ for 27 degrees of freedom. The errors are computed by adding in quadrature the statistical errors for the data and the Monte Carlo.

5. Signal efficiency

The signal efficiency cannot be calculated exactly because the branching ratios of the various decay modes of b -hadrons via the $b \rightarrow s\gamma$ decay are not well known. We have calculated the efficiencies for the most probable exclusive channels of the B meson. The b -baryons are not investigated and not included in the calculation of the limit. The considered exclusive decays, the average multiplicity of the jet, $\langle k_j \rangle$, and the detection efficiency are shown in table 1. The listed decay modes contribute the largest fraction to the total decay modes of the $b \rightarrow s\gamma$. The decay channels differ in the spin and the mass of the strange resonance. Within the uncertainties, the efficiencies are insensitive to the decay modes. The observation that the average number of charged particles is rather independent is understood by the similar decay pattern of the strange states and by the "diluting" effect of the fragmentation. We do not attempt to reweight the efficiencies. A conservative estimate for the efficiency is given by the smallest value in table 1. In the following, we consider the signal detection efficiency:

Table 1

Average multiplicity of the jet closest to the photon, $\langle k_j \rangle$, and selection efficiency, ϵ (%), for different decay modes. (The antiparticle and charge conjugate modes are understood.) The errors are statistical only.

Decay mode	$\langle k_j \rangle$	ϵ (%)
$B^0 \rightarrow K^{*0}(892)\gamma$	3.25 ± 0.04	6.3 ± 0.7
$B^\pm \rightarrow K^{*\pm}(892)\gamma$	3.45 ± 0.04	6.9 ± 0.7
$B^0 \rightarrow K_1^0(1270)\gamma$	3.61 ± 0.07	6.6 ± 0.7
$B^0 \rightarrow K_2^{*0}(1430)\gamma$	3.63 ± 0.05	5.2 ± 0.6
$B^+ \rightarrow \bar{K}_2^{*+}(1430)\gamma$	3.58 ± 0.05	7.6 ± 0.7
$B^0 \rightarrow K_3^{*0}(1780)\gamma$	3.31 ± 0.03	5.6 ± 0.6
$B_s \rightarrow \phi\gamma$	3.48 ± 0.05	7.0 ± 0.7

$$\epsilon_s = 5.2 \pm 0.7(\text{stat.})\% \quad (3)$$

6. Results

After all cuts 88 events remain in the data while 85.9 ± 9.0 are expected from background. The background must be subtracted from the data to extract a limit on the signal. This is a delicate task for the absolute knowledge of the background is intrinsically uncertain. We are reassured by the observation that after the rescaling of the JETSET sample at an early stage of the selection, the data and the Monte Carlo distributions exhibit similar behaviors when more stringent cuts on the electromagnetism and on the signal selection are applied. The Monte Carlo samples from HERWIG and JETSET are added for the estimation of the final background amounting to a total of about 1340 K events, to be compared with 930 K data events.

Using Poisson statistics, the upper limit at the

90% C.L. is 18.6 events. Due to the subtraction of the background from the Monte Carlo prediction, source of systematic errors are investigated. They can be divided in two classes:

(a) systematics due to approximations made in the Monte Carlo generator and in the detector simulation. They induce uncertainties in the physical distributions, as for instance, the distribution of tracks in a jet and the opening of the particles in a jet;

(b) systematics induced by an overall normalization of the background, like the actual number of π^0 's from fragmentation.

The first source of systematic can be expressed as an error on the estimation of the signal and background efficiencies. From the general agreement between the data and the Monte Carlo distributions, a relative systematic error of 2.3% is derived. This includes 2.0% error from the usage of the electromagnetic χ^2 . To understand the effects of these errors on the limit, we vary the selection cuts and calculated the upper limit for the signal in each case. The results are

Table 2

Effect of changing the cuts on the 90% C.L. upper limit. N_{data} is the number of events in data, N_{MC} is the number of expected events, N_{upper} is the upper limit on the expected number of signal events and ϵ_s is the signal detection efficiency. The statistical error on ϵ_s is about $\pm 0.7\%$.

Cut	N_{data}	N_{MC}	N_{upper} (90% C.L.)	ϵ_s (%)
$\chi^2 < 14$	95	96.6	16.80	5.3
$\chi^2 < 8$	80	73.3	20.87	4.9
$\sum_9 / \sum_{25} < 0.98$	116	108.5	24.55	5.6
$\sum_9 / \sum_{25} < 0.995$	70	66.5	17.70	4.9
$ \cos \theta_{\text{thr}} < 0.5$	54	52.2	14.68	3.4
$ \cos \theta_{\text{thr}} < 0.95$	100	100.6	17.80	5.5
jet multiplicity < 6	130	142.0	14.95	7.2
jet multiplicity < 4	46	37.0	19.25	2.5
jet multiplicity < 3	12	11.2	7.70	0.9
$-0.5 < \cos(\theta^*) < 0.5$	86	80.5	20.63	5.0
$0 < \cos(\theta^*) < 0.5$	62	48.4	25.47	2.9
$-0.8 < \cos(\theta^*) < 0$	26	36.0	6.2	2.3
$4 < \hat{m}_B$; $1.8 < E_\gamma^*$, no p_t cut	118	121.2	17.55	7.0
$2 < \hat{m}_B < 9$; no E_γ^* , p_t cut	192	207.9	17.11	9.2
$5 < \hat{m}_B < 6$; no E_γ^* , p_t cut	41	29.8	21.55	2.9

shown in table 2. The number of events in the data and the number of expected events from the Monte Carlo are always consistent.

The fragmentation effects on the amount of π^0 and η background are estimated by noticing that out of the 85.9 ± 9.0 events expected, there are 31.1 ± 5.5 which come from the misidentification of energetic neutral vector mesons decayed into photons. The rate of this fragmentation debris induces a systematic error of about 10%. The effects on the upper limit of changing the number of pions and etas in the Monte Carlo is shown in table 3. The limit increases to 20.80 events when the number of pions and etas are decreased by 10%. For comparison, a global shift of the background normalization by 5% gives approximately the same result. As expected, this is an important source of background for the signal.

Finally, to check the sensitivity of the limit on the detector simulation errors, the energy and angular resolution of the BGO and of the hadron calorimeter are changed in the simulation. As shown in table 4, no effect is observed. The resolution of the thrust axis is however an important parameter as the analysis presumes this direction to estimate the direction of flight

Table 3
Effect of increasing/reducing the background rate. N_{upper} is the upper limit.

Change	N_{MC}	N_{upper} (90% C.L.)
π^0, η rate shift +10%	89.0	16.21
π^0, η rate shift -10%	82.8	20.80
global background shift +5%	90.2	15.67
global background shift -5%	81.6	21.56

Table 4
Effect of artificially changing the simulation of detector effects to show the sensitivity/insensitivity to the imperfections of the simulation. N_{MC} is the number of expected events and ϵ_s is the signal detection efficiency. The changes represent a doubling of the measured (and simulated) resolutions. The statistical errors on the efficiencies are about $\pm 0.7\%$.

Artificial change	N_{MC}	ϵ_s (%)
BGO energy resolution ($\rightarrow 2\%$)	84.2	5.1
BGO angular resolution ($\rightarrow 3$ mrad)	87.1	4.7
HCAL energy resolution ($\rightarrow 110\%/\sqrt{E_{\text{jet}}}$)	81.0	4.9
thrust axis smearing (add 25 mrad in quadrature in θ and ϕ)	83.6	3.5

of the b -hadron. An unrealistic smearing of the thrust axis of 25 mrad in quadrature in both θ and ϕ reduces the efficiency to 3.5%. An absolute systematic error of 0.5% on the efficiency is assigned due to the resolution of the thrust axis.

The number of hadrons corresponding to the data sample is $N_h = 973733 \pm 987$ (stat.) ± 7345 (syst.), where the systematic error on the number of hadrons is estimated to be 0.75%. The branching ratio of the process $Z^0 \rightarrow b\bar{b}$ is taken as $\Gamma_{b\bar{b}}/\Gamma_h = 0.219 \pm 0.008$ [18]. The fragmentation fractions are taken from the JETSET Monte Carlo and are $\text{Br}(b \rightarrow B^0) = 40.8\%$, $\text{Br}(b \rightarrow B^\pm) = 39.6\%$, $\text{Br}(b \rightarrow B_s^0) = 12.1\%$ and $\text{Br}(b \rightarrow b\text{-baryon}) = 7.5\%$. An error of $\pm 2\%$ is assumed on these values. Since the b -baryon decay was not examined, this sample is neglected for the calculation of the limit. The number of B mesons is $N_B = 2 \cdot \text{Br}(b \rightarrow B^0, B^\pm, B_s^0) \cdot \Gamma_{b\bar{b}}/\Gamma_h \cdot N_h = 394508 \pm 17009$. To include the systematic error in the determination of the upper limit, a pessimistic prescription which consists on subtracting the absolute systematic error from the signal efficiency ϵ_s is used. The sources of systematic errors are summarized below:

- 2.3% relative uncertainty in the Monte Carlo simulation of the detector which includes 2.0% from the χ^2 evaluation.
 - 0.5% absolute uncertainty from the thrust axis direction resolution and energy and angular resolutions of BGO and hadron calorimeter.
 - 4.3% absolute error on the number of B mesons N_B where the dominant contribution of 3.7% comes from the branching ratio $\Gamma_{b\bar{b}}/\Gamma_h$.
- The limit is therefore evaluated with $N_B^{\text{sys.}} = 377499$ and with the upper value $N_{\text{upper}}^{\text{sys.}} = 20.80$ which includes a 10% decrease in the number of π^0 's, η 's and

an efficiency $\epsilon_S^{\text{sys}} = 4.58\%$. The limit with the systematic error included is then

$$\text{Br}(b \rightarrow s\gamma) < 1.20 \times 10^{-3}$$

at 90% C.L. (with syst. error) (4)

7. Conclusion

A search for the $b \rightarrow s\gamma$ decay was performed using an integrated luminosity of 37 pb^{-1} at $\sqrt{s} \approx m_Z$. No evidence for a signal was found. The inclusive search was used to set an upper limit on the $b \rightarrow s\gamma$ reaction at $\text{Br}(b \rightarrow s\gamma) < 1.20 \times 10^{-3}$ at the 90% C.L. This result is consistent with the Standard Model expectation. It is also compatible with the preliminary inclusive upper limits obtained by CLEO [19].

Acknowledgement

We wish to express our gratitude for the CERN accelerator divisions for the excellent performance of the LEP machine. We acknowledge the contributions of all the engineers and technicians who have participated in the construction and maintenance of this experiment. Those of us who are not from member states thank CERN for its hospitality and help.

References

- [1] J. Ellis, M.K. Gaillard, D.V. Nanopoulos, Nucl. Phys. B 109 (1976) 213; B 100 (1975) 313.
- [2] A. Salam, Elementary Particle Theory, ed. N. Svartholm (Almqvist and Wiksell, Stockholm, 1968) 367; S. Weinberg, Phys. Rev. Lett. 19 (1967) 1264; P.W. Higgs, Phys. Rev. 145 (1966) 1156; Phys. Rev. Lett. 13 (1964) 508; F. Englert and R. Brout, Phys. Rev. Lett. 13 (1964) 321; A. Salam and J.C. Ward, Phys. Lett. 13 (1964) 168; P.W. Higgs, Phys. Lett. 12 (1964) 132; J. Goldstone, A. Salam and S. Weinberg, Phys. Rev. 127 (1962) 965; S.L. Glashow, Nucl. Phys. 22 (1961) 579; J. Goldstone, Nuovo Cimento 19 (1961) 154.
- [3] J.L. Hewett, Phys. Rev. Lett. 70 (1993) 1045.
- [4] V. Barger, M.S. Berger and R.J.N. Phillips, MAD/PH/730, RAL-92-072 (1992); M. Misiak, Phys. Lett. B 269 (1991) 161; A. Ali and T. Mannel, Phys. Lett. B 264 (1991) 447; P. Cho and B. Grinstein, Nucl. Phys. B 365 (1991) 279; V. Barger, J.L. Hewett and R.J.N. Phillips, Phys. Rev. D 41 (1990) 3421; B. Grinstein, R. Springer and M.B. Wise, Nucl. Phys. B 339 (1990) 269; W.S. Hou and R.S. Willey, Phys. Lett. B 202 (1988) 591; S. Bertolini, F. Borzumati and A. Masiero, Phys. Rev. Lett. 59 (1987) 180.
- [5] R. Barbieri and G.F. Giudice, CERN-TH.6830/93, March 1993; S. Bertolini, F. Borzumati and A. Masiero, Nucl. Phys. B 353 (1991) 591; S. Bertolini, F. Borzumati, A. Masiero and G. Ridolfi, Nucl. Phys. B 294 (1987) 321.
- [6] S.L. Glashow and E.E. Jenkins, Phys. Lett. B 196 (1987) 233.
- [7] L. Susskind, Phys. Rep. 104 (1984) 181; H.W. Haber and G.L. Kane, Phys. Rep. 117 (1985) 75; G. 't Hooft, Recent Developments in Gauge Theories, Proceedings of the NATO Advanced Summer Institute (Cargèse, 1979).
- [8] ARGUS Collab., H. Albrecht et al., Phys. Lett. B 229 (1989) 304; CLEO Collab., P. Avery et al., Phys. Lett. B 223 (1989) 470; CRYSTAL BALL Collab., T. Lesiak et al., Z. Phys. C 55 (1992) 33.
- [9] P. Kim et al., CLNS 93/1212 (CLEO 93-06) (June 1993), submitted to Phys. Lett.
- [10] A. Ali and C. Greub, Phys. Lett. B 259 (1991) 182; Z. Phys. C 49 (1991) 431.
- [11] L3 Collaboration, B. Adeva et al., Nucl. Instr. and Meth. A 289 (1990) 35.
- [12] T. Sjöstrand, Z Physics at LEP 1, eds. G. Altarelli et al., CERN Report CERN-89-08, Vol. 3 (1989) 143; T. Sjöstrand and M. Bengtsson, Comput. Phys. Commun. 43 (1987) 367.
- [13] G. Marchesini et al., Comput. Phys. Comm. 67 (1992) 465; G. Marchesini and B. Webber, Nucl. Phys. B 310 (1988) 461.
- [14] L3 Collab., O. Adriani et al., Phys. Lett. B 292 (1992) 472.
- [15] JADE Collab., S. Bethke et al., Phys. Lett. B 123 (1988) 235.
- [16] C. Peterson, D. Schlatter, I. Schmitt and P. Zerwas, Phys. Rep. 97 (1983) 31.
- [17] L3 Collab., B. Adeva et al., Phys. Lett. B 261 (1992) 177.
- [18] L3 Collab., O. Adriani et al., Phys. Lett. B 307 (1993) 237; L3 Collab., B. Adeva et al., Phys. Lett. B 261 (1991) 177.
- [19] CLEO Collab., E. Thorndike et al., talk given at the 1993 Meeting of the American Physical Society (Washington, DC, April 1993).